Journal of Civil Engineering and Construction 2025;14(3):136-156
https://doi.org/10.32732/jcec.2025.14.3.136

Investigation of Hysteresis Behaviour for Frames with and Without Infill Masonry Concrete Block Wall in Various Aspect Ratios

Ali H. Omar [1,*], Esamaddin Mulapeer[2], Gharbi M. Saadi[3]

1. Highway & Bridge Engineering Department, Erbil Technical Engineering College, Erbil Polytechnic University, Erbil, Iraq
2. Civil Engineering Department, Faculty of Engineering, Tishk International University, Erbil, Iraq
3. Civil Engineering Department, Erbil Technical Engineering College, Erbil Polytechnic University, Erbil, Iraq
E-mail: Ali.H.Omar@Outlook.com

Received: 14 May 2025; Accepted: 26 July 2025; Available online: 5 August 2025

Abstract: This study investigates the hysteresis behavior of single-story reinforced concrete frames with and without infill masonry walls under cyclic loading, focusing on understanding the influence of infill masonry walls and geometric properties, including aspect ratios and story heights, on their structural performance. This research was motivated by required improvements in seismic resilience and safety of reinforced concrete structures. The analysis evaluated parameters like hysteresis behavior, load-carrying capacity, energy dissipation, ductility, and degradation. The analysis reveals that infill walls significantly enhance load-carrying capacity and energy dissipation but reduce ductility, particularly in taller frames. Frames with infill walls exhibited up to 553% higher load-carrying capacity compared to bare frames, while ductility decreased by up to 78% in taller frames. Aspect ratios also played a critical role, with larger ratios improving structural performance. These findings underscore the importance of considering infill walls and geometric properties in seismic design and retrofitting strategies to enhance the resilience of reinforced concrete structures in earthquake-prone regions.
Keywords: Hysteresis behaviour; Infill walls; Concrete block; Aspect ratio; Energy dissipation.

1. Introduction

The examination of hysteresis behavior in RC frames, both with and without infill masonry walls, has garnered substantial attention within the field of structural engineering. This focus is particularly relevant in the context of seismic performance, where understanding the interaction between frames and infill masonry walls is critical for assessing the resilience of structures during dynamic events, such as earthquakes. The complex interplay between these elements profoundly influences the structural response, failure modes, load-bearing capacity, energy dissipation, and overall stability, thus shaping the design and safety of earthquake-resistant buildings. RC frames represent one of the most common structural systems used in low-rise building construction across urban environments.

These systems are favored for their ability to accommodate architectural flexibility, enabling the creation of functional and aesthetically pleasing spaces. Within these RC frames, the gaps between columns—known as structural bays—are frequently filled with infill masonry walls, composed of various materials such as concrete blocks, clay bricks, and concrete bricks. Although these infill masonry walls are not considered primary structural components, their interaction with the RC frames significantly impacts the system's behavior under seismic loading. This interaction can alter the frame's failure mechanisms, potentially changing the expected performance of the entire structure during extreme events, as emphasized by [1]. Therefore, the seismic design of buildings must account for the effects of infill masonry walls to avoid unexpected structural failures.

In conventional design practices, it is generally assumed that the seismic shear forces are primarily resisted by the frame elements, while the infill masonry walls are considered non-structural. However, due to the inherent stiffness of the infill masonry walls, a portion of the seismic load is transferred to these walls, which can redistribute forces within the structural system. This transfer of forces results in additional demands on the RC frame, potentially leading to shear failure and compromising the safety of the entire structure, as noted by [2].

The seismic response of buildings with infill masonry walls has been extensively studied through observations of earthquake-induced damage, including studies by [3,4], example shown in Figure 1. These investigations reveal that the presence of infill masonry walls can dramatically alter the failure modes of RC frames, highlighting the need for a deeper understanding of frame-wall, which often results in non-standard and unpredictable failure mechanisms.

Figure 1. Infill masonry walls performance at Wenchuan Earthquake [3].

Experimental research has advanced the understanding of infill-wall in RC frames through targeted investigations. Early studies by [5-7] established foundational insights into the in-plane behavior of infilled frames, demonstrating that infill walls significantly alter stiffness and failure modes. Subsequent work by [8,9] expanded this knowledge to frames with openings, revealing how geometric discontinuities compromise infill effectiveness. Meanwhile, [10,11] investigated unconventional infill materials such as autoclaved aerated concrete (AAC), highlighting material-specific differences in energy dissipation. Recent studies, including those by [12,13], have focused on progressive collapse mechanisms, emphasizing the role of infills in redistributing forces after column failure. Complementing these efforts, [14,15] explored retrofitting strategies, underscoring the need for models that account for infill-frame synergies. Despite these advancements, the majority of studies—such as those by [16 - 18]—have prioritized traditional small-unit masonry (e.g., clay bricks), leaving a critical gap in understanding the behavior of modern large-format concrete block infills under varying geometric configurations.

Recent advancements in analytical modeling have enabled more sophisticated representations of infill masonry walls in structural analyses [19-25]. [26] developed a simplified macro-model to capture the out-of-plane behavior of infill masonry walls, emphasizing the need for continued exploration of the relationship between frames and infill masonry walls. Their work also introduced drift-based fragility functions for infill masonry walls subjected to in-plane loads, derived from an extensive experimental dataset. This model contributes to a deeper understanding of seismic performance and offers a framework for predicting the behavior of infill masonry wall systems. However, the macroelement modeling approach simplifies infill wall behavior to global in-plane effects and does not explicitly resolve localized damage mechanisms such as block cracking or mortar joint sliding. While this simplification enables computationally efficient analysis, future studies incorporating detailed finite-element models or experimental validation are recommended to investigate localized damage phenomena [26-28].

[29] extended the analysis of RC frames with unreinforced infill masonry walls by incorporating both in-plane and out-of-plane relationship. Their research highlighted the importance of accounting for the combined effects of these two modes of failure to accurately predict the seismic performance of RC frames. Additionally, [30] introduced a computationally efficient strut model that captures the nonlinear dynamic response of infill masonry walls under in-plane loading. This model enhances the accuracy and practicality of incorporating infill masonry walls into large-scale structural analysis, providing engineers with valuable tools for predicting seismic behavior.

Further research into the role of infill masonry walls has demonstrated their significant impact on structural performance, particularly in terms of load-bearing capacity and stiffness. [31] found that infill masonry walls increase the load-carrying capacity of RC frames, contributing to the overall strength of the building when subjected to extreme events like earthquakes. Their research emphasizes that infill masonry walls must be considered in the seismic design process, as their relationship with the RC frame can drastically alter the structural response.

[29] also observed that the inclusion of infill masonry walls not only enhances the structural strength but can also change the collapse mechanisms under strong ground motions. This indicates that the failure modes of RC frames with infill masonry walls can be complex and difficult to predict, further highlighting the importance of understanding these relationship in seismic design. Infill masonry walls also play a crucial role in energy dissipation, particularly during seismic events. [32] demonstrated that the strategic use of infill masonry wall materials can enhance the energy absorption capacity of the structure, which is vital for mitigating seismic damage. Understanding the hysteresis behavior of RC frames, especially in relation to different aspect ratios and wall heights, is essential for improving design practices aimed at enhancing seismic resilience.

[33] conducted an extensive review of the relationship between infill masonry walls and RC frames, concluding that macro-modeling approaches are necessary to accurately capture the complexities of energy dissipation and stiffness degradation under cyclic loading. These findings suggest that traditional analytical models may not fully

account for the complex behaviors introduced by infill masonry walls, particularly in terms of their contribution to energy dissipation and their impact on overall system stability.

The seismic performance of reinforced concrete (RC) frames with masonry infills has been a focal point of research in recent years, underscoring the complexities introduced by various modeling techniques and material properties. [34] highlighted the critical impact of infill variability and modeling uncertainty on the seismic loss assessment of existing RC school buildings, emphasizing the need for comprehensive evaluations that account for both structural and non-structural components. Similarly, [35] explored the quantification of uncertainties affecting the seismic fragility functions of masonry-infilled RC frames, revealing that different modeling approaches can yield significantly varied fragility functions, thus impacting seismic risk assessments. The importance of the aspect ratio of infills in influencing both in-plane and out-of-plane effects was examined by [36], who found that the infill's geometry plays a crucial role in its behavioral response under seismic loads, leading to variations in damage states. Additionally, [37] conducted a parametric study that underscored how the infill's characteristics and distribution directly affect the seismic performance of RC frames, corroborating the notion that certain frame types are more susceptible to adverse infill effects. These studies collectively reinforce the significance of considering infill properties and uncertainties in modeling efforts to achieve more accurate assessments of the seismic behavior of RC structures.

Recent research has underscored the critical role of masonry infill walls in enhancing the seismic performance of reinforced concrete (RC) structures. For instance, [38] highlights that uniform distribution of infill walls significantly improves lateral stiffness and reduces inter-story drift, crucial factors for mitigating earthquake damage in multi-story buildings with shear walls. Also, investigated the presence of soft story conditions in RC structures and demonstrated that infill walls can lead to substantial increases in structural resistance, particularly in configurations with weak column-strong beam design. Additionally, the study by [39] illustrates how varying infill wall distributions affect collapse probabilities, indicating that symmetric arrangements enhance building safety by lowering the likelihood of structural failure during seismic events. [40] further emphasize the need for accurate modeling of infill contributions to the overall structural response, revealing that variability in infill properties can significantly influence seismic loss assessments. Lastly, [41] explores the implications of modeling uncertainties in infilled RC frames, noting that these uncertainties can lead to substantial variations in fragility functions, thereby affecting the reliability of seismic performance estimates. This body of work collectively emphasizes the importance of incorporating detailed infill modeling in the seismic analysis of RC structures, particularly through fiber-based approaches that accurately simulate the nonlinear behavior of both infill and structural elements.

Recent advancements in the modeling and experimental characterization of infilled RC frames have significantly enhanced the understanding of infill-wall under seismic loading. [42] proposed a pioneering macro-model capable of simulating the coupled in-plane and out-of-plane behavior of unreinforced and retrofitted masonry infills, addressing a critical gap in bidirectional analysis. Complementing this, [43] conducted substructured pseudodynamic tests on a full-scale five-story RC building with masonry infills, establishing empirical damage thresholds and quantifying system-level under realistic seismic demands. Concurrently, [44] employed finite-element simulations to investigate the local effects of autoclaved aerated concrete (AAC) infills on RC frames, revealing distinct stress distributions and failure mechanisms compared to conventional masonry.

The majority of existing studies have focused on material properties, number of stories, and various types of structural elements, including steel and concrete frames while examining hysteresis behavior through both experimental research and analytical simulations. However, most of these studies have traditionally employed smaller infill masonry wall units, such as clay and concrete bricks, which differ from the larger concrete blocks now widely used in modern construction. These larger blocks offer advantages in terms of ease and speed of construction but also exhibit different mechanical properties that may influence the behavior of RC frames during extreme events.

While extensive research has been conducted on the seismic performance of RC frames with infill walls, most studies have traditionally focused on smaller infill units, such as clay or concrete bricks, which differ significantly from the larger concrete blocks now prevalent in modern construction. These larger blocks offer advantages in terms of construction efficiency but exhibit distinct mechanical properties that may influence the structural behavior under seismic loading. Furthermore, the influence of geometric properties, particularly aspect ratios and frame heights, on the hysteresis behavior of RC frames with these larger infill blocks has not been thoroughly investigated. This study addresses these gaps by (1) analyzing the hysteresis behavior of RC frames with and without infill walls made of larger concrete blocks, (2) evaluating the impact of varying aspect ratios and frame heights on structural performance, and (3) assessing the RC frames and infill walls under extreme loading conditions. By focusing on modern construction materials and geometric parameters, this research provides novel insights into the seismic design and retrofitting of RC structures, offering practical guidance for engineers working in earthquake-prone regions.

It is crucial to recognize the limitations of this study even though it offers insightful information about the hysteresis behavior of reinforced concrete frames with and without infill masonry walls. This work is limited to analytical studies that model the behavior of the structure under cyclic loading using numerical simulations.

In light of this, experimental studies are not included in this study, despite the fact that they are essential for confirming analytical models and capturing the entire spectrum of complex relationships that occur between frames and infill masonry walls during seismic events. More reliable information on topics like material behavior, cracking patterns, and energy dissipation—aspects that are challenging to fully replicate in a strictly analytical framework—may be obtained through experimental testing. To ensure a thorough understanding, the results may need to be verified through physical experiments, so the study's findings should be interpreted in light of these limitations.

2. Investigation program

This research presents a comprehensive analytical investigation of structural frames by SeismoStruct software [45], both with and without infill masonry walls, across a range of aspect ratios.

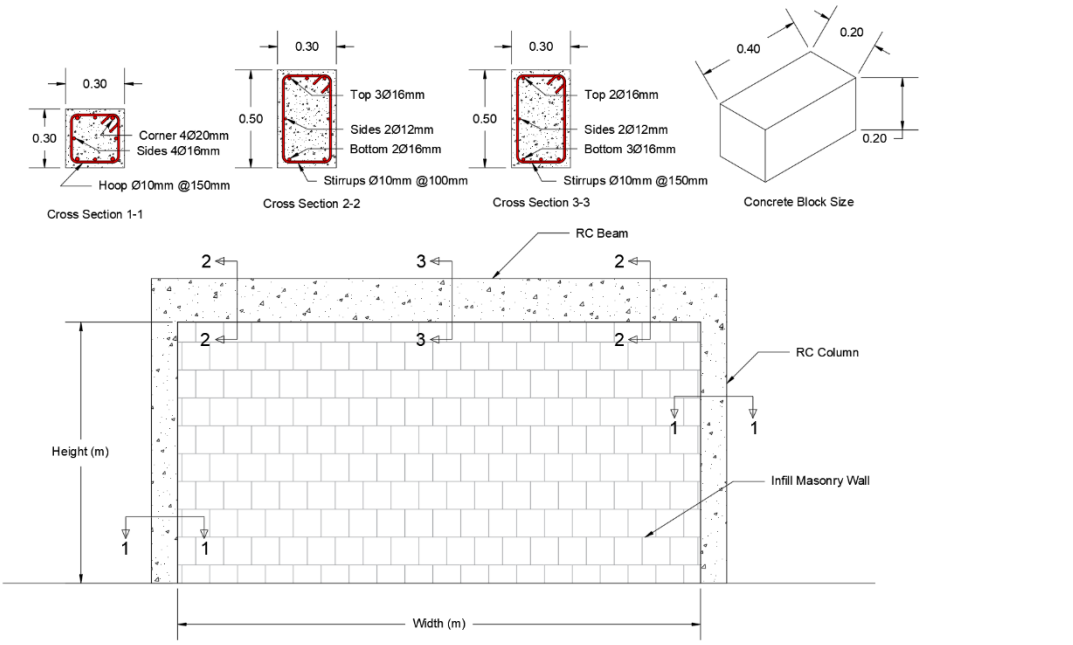

Figure 2. Infill masonry wall arrangement and frame reinforcement detail (units are in meters).

The primary goal of this study is to investigate the impact of varying aspect ratios on the hysteresis behavior of infill masonry walls, which are critical components in the overall structural performance during seismic events. Hysteresis behavior, which describes the energy dissipation characteristics of a structure under cyclic loading, is essential for understanding how infill masonry walls contribute to the seismic resilience of a building. Table 1 systematically presents the model names, along with the corresponding dimensions height, and width of the walls utilized in this study. This data forms the basis for a comparative analysis aimed at identifying patterns and correlations between aspect ratio and structural response.

2.1 Geometric properties

The geometric configuration of the frames was meticulously designed to adhere to the specified dimensions, as detailed in Table 1.

Each column within the frames has a cross-sectional area of 300 mm x 300 mm, reinforced with a sophisticated arrangement of steel rebars to ensure structural integrity and resistance to loading. Specifically, the columns are reinforced with four 20 mm diameter rebars positioned at the corners, providing critical support against lateral forces. Additionally, four 16 mm diameter rebars are placed along the sides of the columns, further enhancing the load-bearing capacity. The reinforcement scheme includes 10 mm diameter hoops, strategically spaced at 150 mm intervals, to prevent buckling and to confine the concrete, thereby improving the column's ductility and energy absorption capacity.

The beams, integral to the frame's structural system, are reinforced following a precise design to optimize performance under both vertical and lateral loads. The tensile section of the beam is reinforced with three 16 mm

diameter rebars positioned at the bottom center and top ends, which are crucial for resisting tensile forces. In the compression section, two 16 mm diameter rebars are placed at the top center and ends of the bottom, complementing the tensile reinforcement below. Additionally, the central sides of the beam are reinforced with two 12 mm diameter rebars, providing additional stiffness and strength. The stirrups, with a diameter of 10 mm, are spaced at 100 mm intervals at the ends and 150 mm intervals at the center, ensuring that the shear forces are effectively managed and distributed across the beam.

Table 1. Frame models geometric parameters.

No	Description	Group Name	Height (m)	Width (m)	Aspect Ratio	Aspect Ratio W/H	Model Name
1	Without Infill masonry walls	A	3	3	1:1	1	1-1 WOIF-1
2	Without Infill masonry walls		3	4	4:3	1.33	4-3 WOIF
3	Without Infill masonry walls		3	5	5:3	1.66	5-3 WOIF
4	Without Infill masonry walls		3	6	2:1	2	2-1 WOIF
5	Without Infill masonry walls	B	4	3	3:4	0.75	3-4 WOIF
6	Without Infill masonry walls		4	4	1:1	1	1-1 WOIF-2
7	Without Infill masonry walls		4	5	5:4	1.25	5-4 WOIF
8	Without Infill masonry walls		4	6	3:2	1.5	3-2 WOIF
9	With Infill masonry walls	C	3	3	1:1	1	1-1 WIF-1
10	With Infill masonry walls		3	4	4:3	1.33	4-3 WIF
11	With Infill masonry walls		3	5	5:3	1.66	5-3 WIF
12	With Infill masonry walls		3	6	2:1	2	2-1 WIF
13	With Infill masonry walls	D	4	3	3:4	0.75	3-4 WIF
14	With Infill masonry walls		4	4	1:1	1	1-1 WIF-2
15	With Infill masonry walls		4	5	5:4	1.25	5-4 WIF
16	With Infill masonry walls		4	6	3:2	1.5	3-2 WIF

Furthermore, a concrete clear cover of 25 mm has been employed for both the columns and the beam, ensuring durability and protection of the reinforcement against environmental factors. The infill masonry walls, constructed using concrete blocks with dimensions of 400 mm x 200 mm x 200 mm, play a significant role in the overall load-carrying capacity of the frame since it will affect the contact area between the frame and infill masonry wall which later clarified in the modeling section. The configuration and placement of these blocks, as illustrated in Figure 2, are critical for understanding how variations in aspect ratio influence the hysteresis behavior and the overall seismic performance of the structure. This meticulous attention to geometric properties ensures that the study's findings are robust and applicable to real-world scenarios in structural engineering.

2.2 Material properties and modeling

In the analytical modeling of the frame members, including columns and beams, a concrete compressive strength of 30 MPa was utilized. This choice reflects a typical structural grade concrete. The infill masonry wall made from concrete blocks, essential to the composite behavior of the frame, was modeled with a compressive strength of 20 MPa, indicative of standard concrete block units used in construction. The mortar, a critical component that influences the interaction between the masonry infill wall units and the frame, was assigned a compressive strength of 5 MPa. The reinforcement rebars, crucial for the structural integrity and ductility of the frame, were modeled with a yield tensile strength of 420 MPa and an ultimate tensile strength of 640 MPa. These values are consistent with high-strength steel commonly used in RC structures. A comprehensive list of material properties, including those related to elasticity, ductility, and durability, is systematically presented in Table 2 to provide a complete understanding of the materials' performance characteristics.

To accurately represent the nonlinear behavior of concrete under varying load conditions, the modeling approach is employed in the [46] confinement model. This model is particularly well-regarded for its ability to simulate the effects of confinement on concrete's stress-strain behavior, especially under uniaxial compressive loading. The model's implementation was further enhanced by the work of [47-48], who incorporated the model into simulation software, allowing for a detailed representation of concrete's response under cyclic loads. The cyclic behavior, which is critical in seismic analysis, was further refined by integrating the rules and relationships developed by [49]. As shown in Figure 3. These contributions provide a robust framework for understanding the degradation and energy dissipation characteristics of concrete when subjected to repeated loading and unloading cycles, which are typical in seismic events.

For the modeling of the cyclic behavior of the reinforcement rebars, the "Generic Hysteretic Model" was employed [45]. This model is embedded within the structural analysis software [45] and is designed to capture the

complex relationship that occur in materials under cyclic loading, particularly those associated with the pinching effect and material deterioration. The pinching effect, which is a manifestation of the reduced stiffness and energy dissipation during unloading and reloading cycles, is controlled by a pinching factor within the model. This factor ranges from 0, indicating no pinching, to 1, representing a pronounced pinching effect. The model also accounts for four distinct modes of deterioration: strength deterioration, peak stress deterioration, reloading stiffness deterioration, and unloading stiffness deterioration. Each mode is characterized by a deterioration factor, also ranging from 0 to 1, where 0 indicates no deterioration and 1 signifies severe degradation.

Table 2. Material properties.

Parameters	Frame Concrete	Concrete Block	Mortar	Rebar
Compressive Strength (Mpa)	30	20	5	-
Tensile Strength (Mpa)	2.2	1.6	0.5	-
Modules of Elasticity (Mpa)	25743	21019	10509	200000
Strain at Peak Stress (m/m)	0.002	0.002	0.002	-
Yield Strength (Mpa)	-	-	-	420
Yield Strain (m/m)	-	-	-	0.002
Ultimate Strength (Mpa)	-	-	-	640
Ultimate Strain (m/m)	-	-	-	0.12
Rupture Strain (m/m)	-	-	-	0.18
Pinching factor (kpa)	-	-	-	1.0
Deterioration Factor (kpa)	-	-	-	1.0

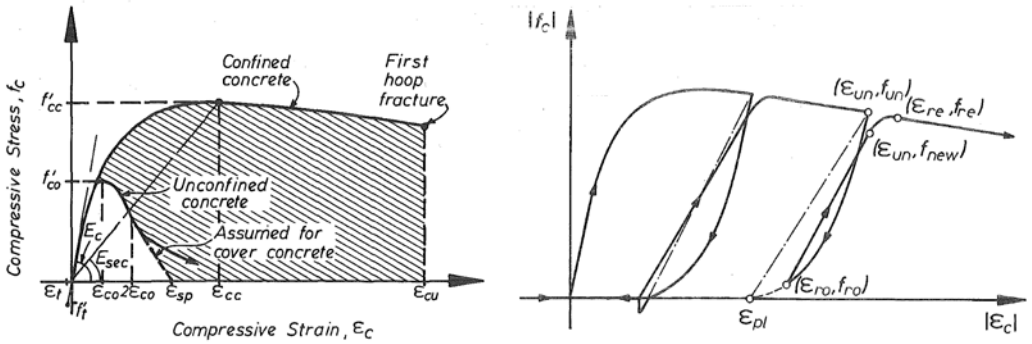

Figure 3. Proposed model for concrete stress-strain relationships [46].

Additionally, the "Generic Hysteretic Model" incorporates several key parameters that define the backbone curve of the material's stress-strain relationship. These include the modulus of elasticity, which determines the initial stiffness of the material; yield strength, which dictates the onset of plastic deformation; peak strain, which represents the maximum strain before failure; peak stress, which is the maximum stress the material can withstand; and residual strength, which indicates the remaining strength after significant damage. These parameters are critical for accurately simulating the nonlinear and inelastic behavior of the reinforcement under seismic loading conditions, ensuring that the model provides a realistic and comprehensive representation of the structural performance.

2.3 Element modeling

For the accurate representation of infill masonry walls in the structural model, the inelastic infill panel element developed by [50] was employed. This element is a sophisticated 4-node infill masonry wall panel specifically designed for framed structures, capturing the global in-plane behavior of the infill walls through equivalent strut elements. While the model accounts for stiffness degradation, energy dissipation, and cyclic strength reduction, localized damage mechanisms such as cracking or crushing of individual masonry blocks are not explicitly resolved. Instead, these effects are represented through phenomenological degradation parameters calibrated to experimental data.

The axial struts follow the infill masonry strut hysteresis model [50], defined by a trilinear backbone curve with the following key parameters:

$$k_e = \frac{E_{inf}.t_{inf}.\sin(2\theta)}{2.l_{diag}} \ (Elastic\ Stiffness) \quad (1)$$

$$F_y = 0.8\, f'_{inf}\ t_{inf} l_{diag} \cos\theta \ \ (Yield\ Strength) \quad (2)$$

$$F_p = 1.0 f'_{inf}\, t_{inf} l_{diag} \cos\theta \;\; (Peak\ Strength) \quad (3)$$

where: E_{inf} Elastic modulus of the infill masonry, t_{inf} Thickness of the infill wall, l_{diag} Diagonal length of the infill panel, θ Angle between the diagonal strut and the horizontal axis, f'_{inf} Compressive strength of the infill masonry. The shear strut follows a bilinear hysteresis rule with strength proportional to the axial compression in the diagonal struts [50]. Cyclic degradation (e.g., stiffness reduction, pinching) was modeled using SeismoStruct's default parameters for concrete block masonry.

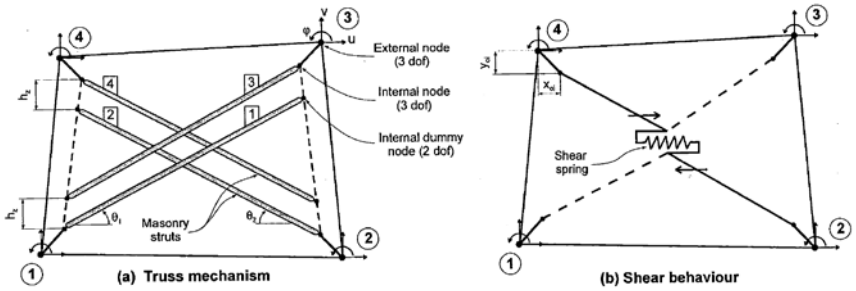

Figure 4. Proposed 4-node panel element for masonry infill frame analysis [50].

The panel is modeled using six strut members, strategically arranged to simulate the mechanical behavior of the infill masonry walls under loading conditions. Each diagonal direction within the panel features two parallel struts that carry axial loads across the diagonally opposite corners of the panel, ensuring the correct transfer of forces within the structure. A third strut is incorporated to handle the shear forces transmitted from the top to the bottom of the panel. This shear-carrying strut is unique in that it only activates when the panel experiences compression along the diagonal, meaning its contribution depends on the deformation state of the panel. The axial load-carrying struts are modeled using the infill masonry wall strut hysteresis model, while the shear strut follows a dedicated bilinear hysteresis rule, providing an accurate representation of the nonlinear behavior of the infill masonry walls under cyclic loading conditions.

Figure 4 illustrates the proposed 4-Node Panel Element for Infill Frame Analysis as developed by [50]. As depicted in the figure, the model includes four internal nodes, which account for the actual points of contact between the frame and the infill masonry walls. These nodes are crucial for considering the width and height of the columns and beams, thereby ensuring an accurate representation of the physical interaction between the frame and the infill masonry wall. Additionally, four dummy nodes are introduced to model the contact length between the frame and the infill masonry wall. The internal forces are then transformed to the four exterior nodes, which are defined in an anti-clockwise sequence to ensure proper connectivity with the frame. This modeling approach allows for a detailed and realistic simulation of the interaction between the infill masonry wall and the surrounding frame, capturing the critical aspects of load transfer and deformation.

For the modeling of the columns and beams, an inelastic force-based plastic hinge frame element was utilized. This element is a 3D beam-column type capable of modeling members of space frames that exhibit both geometric and material nonlinearities. The element's formulation allows for a precise representation of the sectional stress-strain state of the beam-column elements, achieved through the integration of the nonlinear uniaxial material response of individual fibers. The section of each beam and column is subdivided into these fibers, allowing the model to fully account for the spread of inelasticity along the length of the member and across its sectional depth. This approach concentrates inelasticity within a fixed length of the element, as proposed by [51], providing a more accurate depiction of the plastic hinge behavior in structural members.

One of the significant advantages of this force-based plastic hinge formulation is its efficiency in analysis time. Since fiber integration is performed only at the two ends of the member, the computational load is reduced, making the analysis more efficient. Furthermore, this approach offers full control and calibration of the plastic hinge length, which is critical for addressing localization issues. This capability allows for a more refined and accurate modeling of inelastic behavior in structural members, as discussed in studies such as [52]. Figure 5 provides a visual representation of the modeling approach, highlighting the effectiveness of this element in capturing the complex behaviors exhibited by structural frames under various loading conditions.

The limitations of modeling approach in masonry infill walls in this study were simulated using SeismoStruct's Masonry Infill Strut Model, which simplifies the infill panel into an equivalent diagonal strut to capture in-plane stiffness, strength, and cyclic degradation. While this approach effectively models key in-plane behaviors—such as diagonal compression, shear transfer, and hysteresis pinching—it does not account for out-of-plane interactions or localized damage mechanisms (e.g., mortar joint sliding, corner crushing). The strut model relies on empirically

calibrated parameters (e.g., compressive strength, strain limits, cyclic unloading stiffness) derived from experimental data, which may not fully reflect variability in real-world masonry properties or construction quality.

Acknowledging these limitations, the analysis assumes infill walls contribute solely to in-plane resistance, neglecting out-of-plane forces that could arise during bidirectional seismic loading. This simplification may underestimate damage progression and overestimate energy dissipation, particularly in taller frames or panels with low aspect ratios. Future work should integrate advanced finite-element models or experimental testing to address combined in-plane/out-of-plane effects and validate the strut model's assumptions under diverse failure modes.

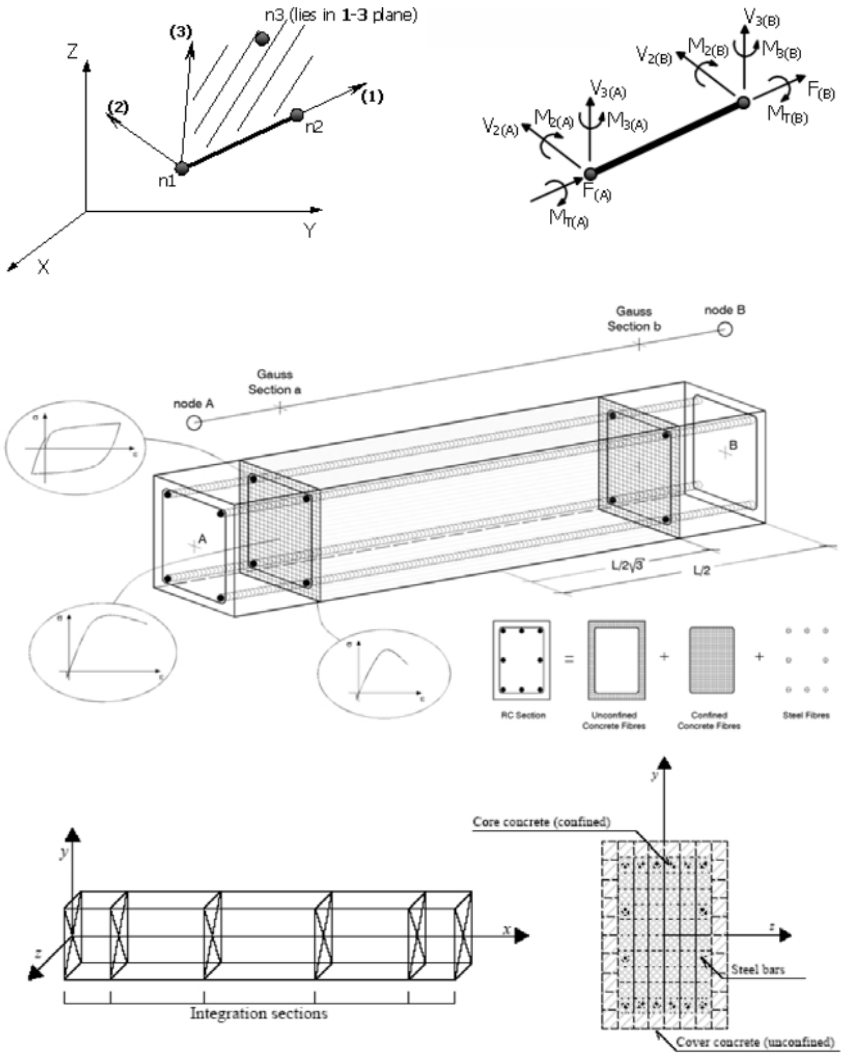

Figure 5. Local axis and fiber integration.

2.4 Loading protocol

The loading protocol employed in this study was carefully designed to simulate the realistic conditions that the structural frame would experience under seismic loading. As illustrated in Figure 6, the schematic of the loading system provides a detailed representation of how the frame was subjected to these forces. The frame was modeled with fixed supports at the base, ensuring that the connection to the ground was rigid and allowing for the accurate simulation of base shear forces. The center of the beam was designated as the control node, a critical point for capturing the deflection measurements throughout the analysis. This location was strategically chosen because it experiences the most significant displacement, making it ideal for assessing the frame's overall deformation behavior. Meanwhile, the bases of the columns were identified as key points for measuring the shear forces, providing insight into how the lateral loads were distributed through the structural elements.

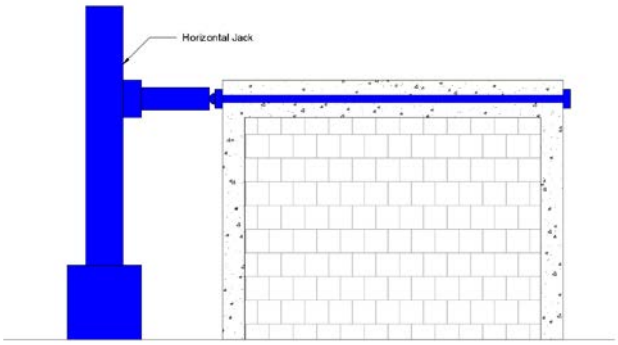

Figure 6. Schematic diagram of the test simulation loading system.

The loading protocol itself was defined by a cyclic behavior, implemented through the use of a static time history analysis. This approach involved applying displacements that varied over a pseudo-time domain, allowing for the simulation of the frame's response to repeated loading and unloading cycles, as would occur during an earthquake. The maximum displacement applied during the analysis was 320 mm, which was selected based on the anticipated performance range of the structure under extreme loading conditions. This displacement was applied incrementally, following the cyclic loading protocol depicted in Figure 7. The cyclic nature of the loading is essential for understanding the hysteresis behavior of the frame, which reflects how the structure dissipates energy and undergoes permanent deformation under cyclic loads.

Figure 6 and Figure 7 provides a visual representation of the test loading system and the cyclic loading protocol. The diagram emphasizes the importance of both the control node and the column base measurements, ensuring that the most critical aspects of the structural response were captured during the analysis. The cyclic loading protocol, with its carefully controlled increments, allows for a detailed examination of the frame's resilience and the potential failure mechanisms that may arise under seismic conditions. This rigorous approach to loading ensures that the study's findings are robust and can be reliably applied to the design and assessment of similar structures in seismic regions.

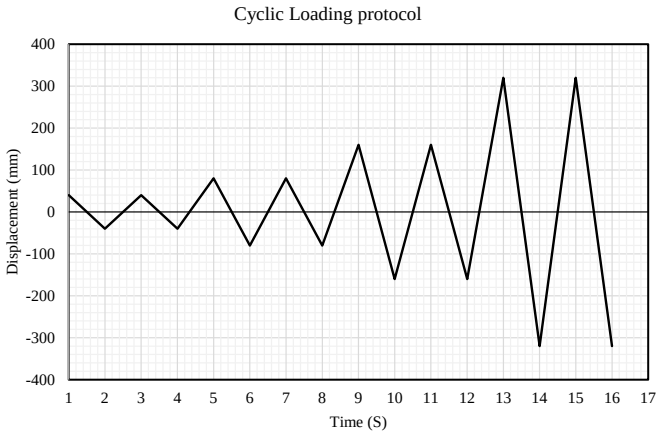

Figure 7. Cyclic loading protocol.

3. Analysis results and discussion

3.1 Hysteresis curves

The hysteresis behavior of a single two-column and one-beam RC frame was examined, focusing on frames with different aspect ratios. The frames were divided into two groups: Group A, with a story height of 3 meters and width-to-height ratios of 1, 1.33, 1.66, and 2, and Group B, with a story height of 4 meters and width-to-height ratios of 0.75, 1, 1.25, and 1.5. These frames were subjected to cyclic lateral loading to evaluate their performance under seismic-like conditions. Despite the differences in aspect ratios and story heights, the hysteresis curves for these frames were found to be remarkably similar, indicating consistent energy dissipation behavior across the different configurations. However, a notable distinction was observed in the load-carrying capacity between the two groups.

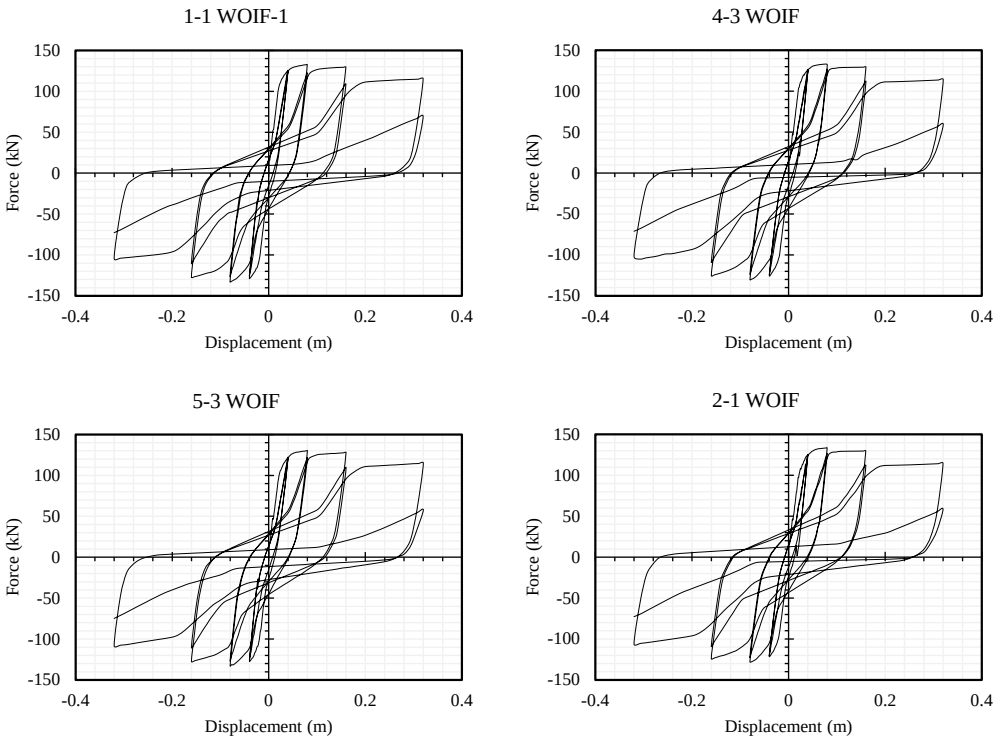

Figure 8. Global hysteresis curves for RC frames without infill masonry walls (Group A, 3m story height).

The hysteresis curve for a typical RC frame, such as those in this study, represents the relationship between lateral displacement (on the X-axis) and the restoring force or base shear (on the Y-axis) during cyclic loading and unloading. The curve typically forms a loop, where the area enclosed by the loop reflects the energy dissipated by the frame during each loading cycle. In RC frames, this energy dissipation occurs due to mechanisms such as concrete degradation, yielding of the steel reinforcement, and other inelastic deformations. The shape of the hysteresis curve provides insights into the frame's stiffness, strength, and overall resilience under repeated loading.

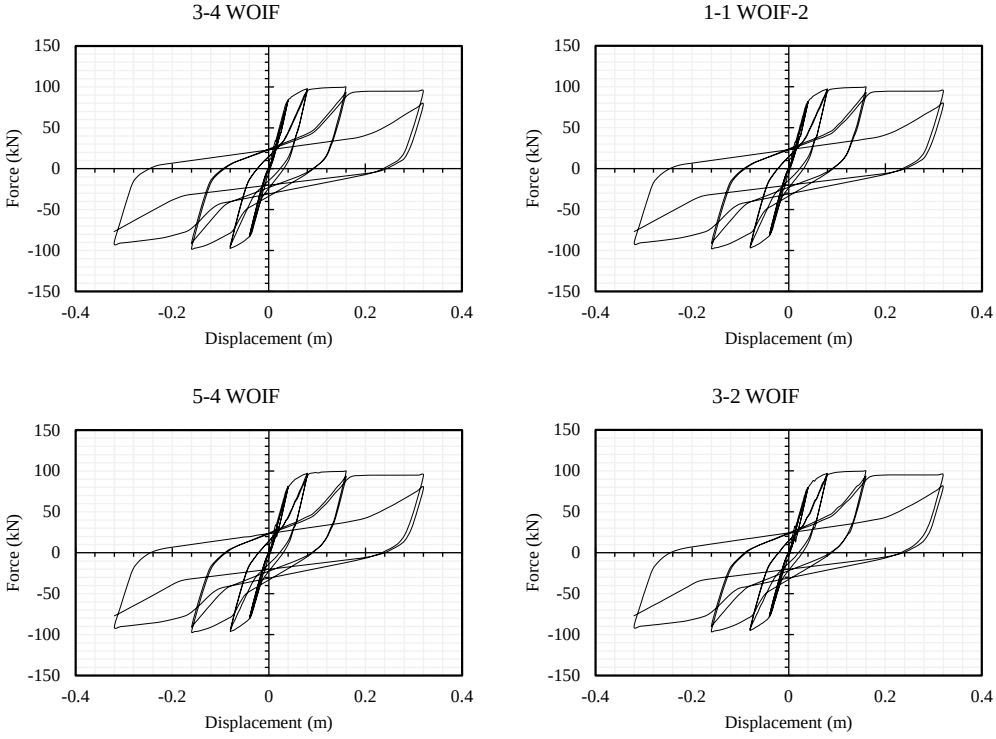

Figure 9. Global hysteresis curves for RC frames without infill masonry walls (Group B, 4m story height).

For the frames in Group A, with a 3-meter story height, the hysteresis curves, as shown in Figure 8, exhibited a higher load-carrying capacity compared to those in Group B, which had a 4-meter story height, with their curves presented in Figure 9. This difference can be attributed to the shorter height of the frames in Group A, which likely contributed to greater structural stiffness and reduced lateral deflections, allowing these frames to sustain higher loads before significant inelastic deformations occurred. The initial portion of the hysteresis curve, representing the loading path, showed a steeper slope for Group A frames, indicating higher stiffness in the elastic range. As the loading continued and the frames entered the inelastic range, the curves began to flatten, reflecting the onset of yielding and plastic deformations. During unloading, the hysteresis curves did not retrace the loading path, a characteristic behavior in RC frames due to the permanent deformations that occur. This results in a pinched loop, which was observed in both groups. However, the extent of pinching was less pronounced in the Group A frames, suggesting that they retained more of their stiffness and energy dissipation capacity even after multiple cycles of loading. The residual deformations after unloading were also smaller for Group A frames, indicating less cumulative damage and a higher potential for withstanding further seismic events.

The hysteresis loops for the Group B frames, with their 4-meter story height and lower width-to-height ratios, were more pinched, and the loops became narrower with successive loading cycles, signifying greater stiffness degradation and lower energy dissipation capacity. This suggests that the taller frames in Group B were more susceptible to damage and permanent deformation under cyclic loading, which could reduce their effectiveness in dissipating seismic energy and increase the risk of failure during a strong earthquake. The results of this study are in well agreement with the experimental RC frame hysteresis curves provided by [53], reinforcing the validity of the findings.

Despite of the Group A and B the hysteresis behavior of RC frames with infill masonry wall panels investigated with varying aspect ratios. These frames were divided into two groups: Group C, with a story height of 3 meters and width-to-height ratios of 1, 1.33, 1.66, and 2, and Group D, with a story height of 4 meters and width-to-height ratios of 0.75, 1, 1.25, and 1.5. The presence of infill masonry walls significantly influenced the hysteresis behavior, with the hysteresis curves for these frames being more pinched compared to those of frames without infill masonry walls. This pinching effect, indicative of greater stiffness degradation and energy dissipation, aligns well with the experimental hysteresis curves provided by [54].

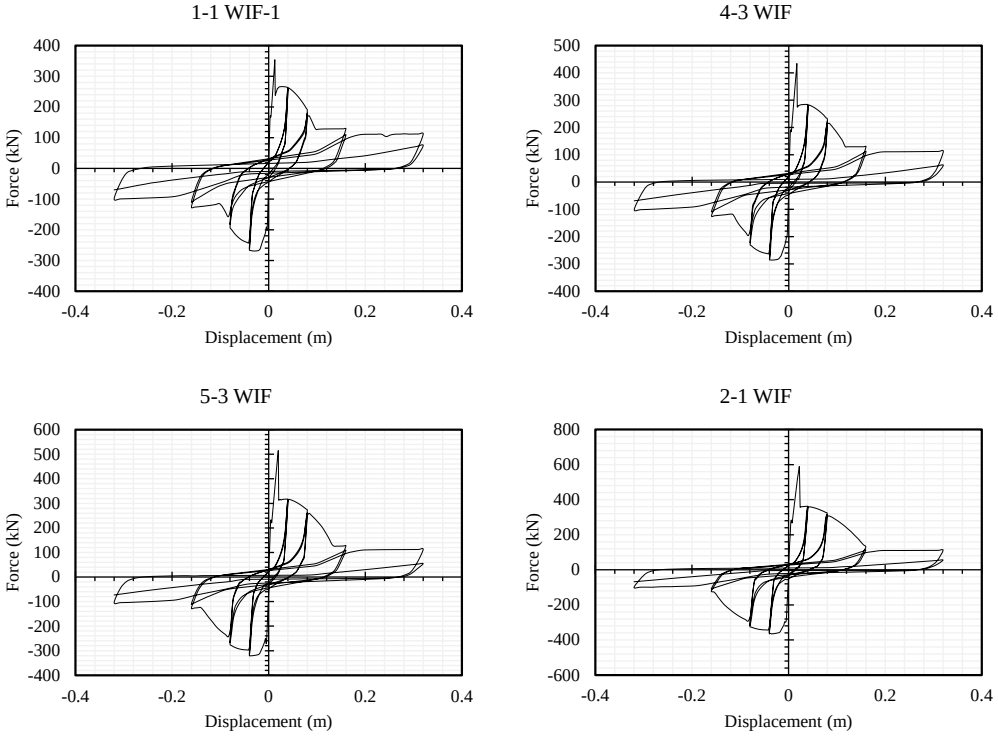

Figure 10. Global hysteresis curves for the frames without infill masonry walls (Group C).

As shown in Figure 10 and Figure 11. At the initial stage of loading, the hysteresis loop exhibited a shuttle shape, indicative of the structure's strong energy dissipation capacity. This shape can be attributed to the high strength and stiffness of the concrete blocks used in the infill masonry walls, which contribute to the overall rigidity of the frame system. The hysteresis curve remained close to the ordinate axis due to the initially high stiffness of the infill masonry walls, signifying a steep initial slope. This steepness reflects the large initial stiffness, meaning

the structure's load-bearing capacity increased rapidly during the early stages of loading. Consequently, the peak bearing capacity of the frames with infill masonry walls was notably higher than those without, emphasizing the significant contribution of the infill masonry walls to the overall strength of the system.

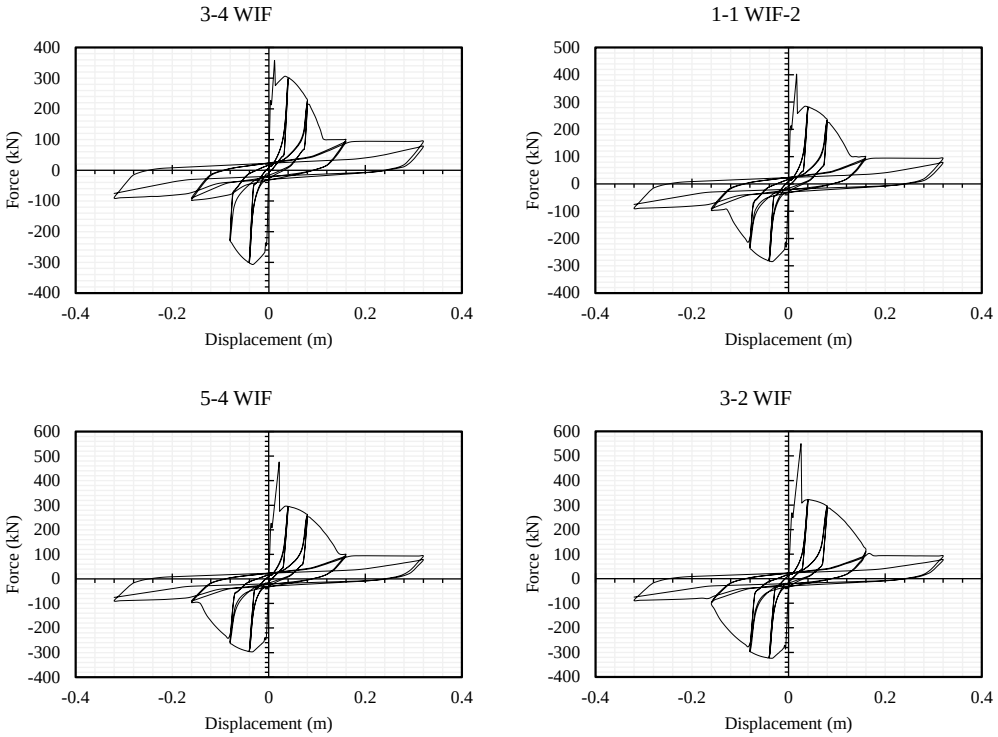

Figure 11. Global hysteresis curves for the frames without infill masonry walls (Group D).

However, as cyclic loading continued and displacement increased, the strong interaction between the infill masonry walls and the RC frame led to degradation in both the frame and the infill masonry wall. This damage altered the shape of the hysteresis loop, which gradually evolved into an "anti-S" shape. This transformation reflects the reduced stiffness and the onset of inelastic behavior as degradation developed and propagated through the structure. The anti-S shape of the hysteresis curve is a clear indication that the specimen began to experience shear damage. The post-peak behavior of the hysteresis loop was characterized by a sharp decline in load-carrying capacity, reflecting the poor deformation capacity of the frame system after shear failure. This rapid decrease in stiffness and strength suggests that while the infill masonry walls provide substantial initial rigidity and strength, they also contribute to a more brittle failure mode once the peak load is exceeded. The height of the infill masonry wall further exacerbated this effect, as seen when comparing specimens 1-1 WIF-1 and 1-1 WIF-2, with story heights of 3 meters and 4 meters, respectively. The 4-meter-high infill masonry wall in 1-1 WIF-2 exhibited different hysteresis characteristics compared to the 3-meter-high panel in 1-1 WIF-1, emphasizing the importance of the infill masonry wall's height in determining the hysteresis behavior and load-carrying capacity.

These findings have important implications for seismic design and retrofitting strategies. The superior performance of frames with lower story heights suggests that in seismic-prone regions, limiting building height or incorporating intermediate stiffening elements in taller structures could enhance seismic resilience. For retrofitting existing structures, the addition of infill walls could significantly improve initial stiffness and load-carrying capacity, but care must be taken to account for the potential for more brittle failure modes at higher displacements.

3.2 Backbone curves

The backbone curves for all 16 specimens, categorized into four distinct groups, are shown in Figure 12. These curves provide a clear visualization of the structural response by tracing the peak points of the hysteresis loops at various stages of cyclic loading. Essentially, the backbone curve is a simplified representation that highlights the key points in the load-displacement behavior of the structure, and it is critical for understanding the nonlinear response of the frames.

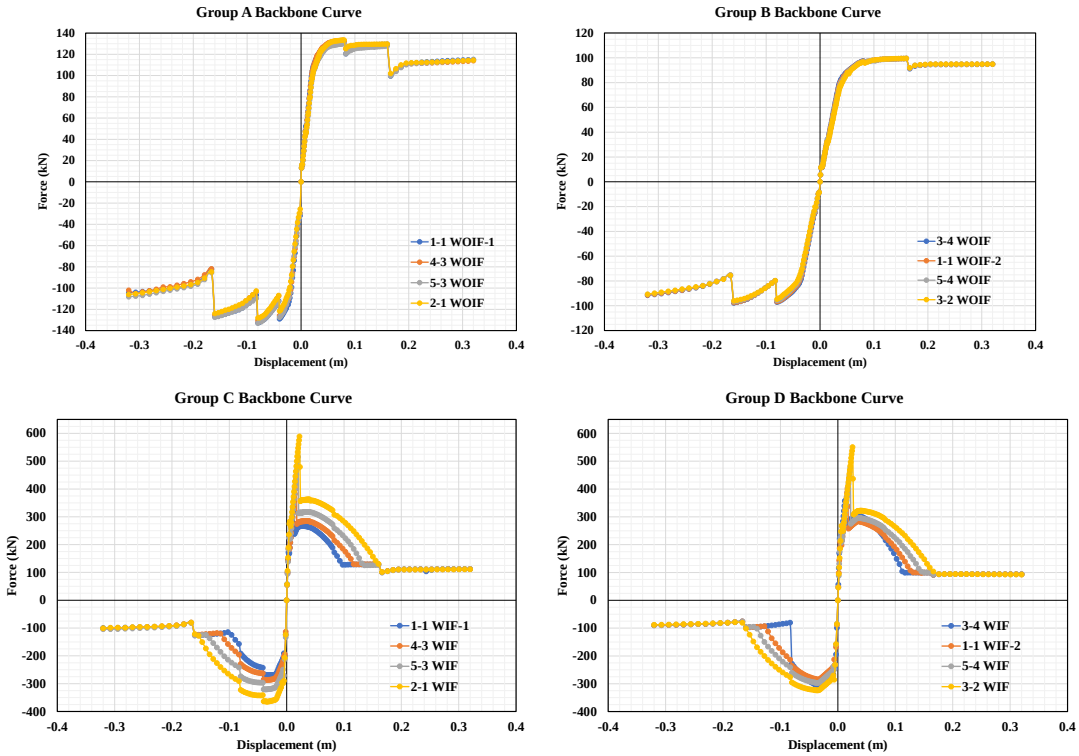

Figure 12. Backbone curves for All 16 specimens a cross four groups (A,B,C,D).

The principal characteristic points—yielding displacement, yielding load, peak load, peak displacement, ultimate load, and ultimate deflection—are listed in Table 3 for both the positive and negative loading directions. To derive these characteristic points, the yielding displacement and load were determined using the equivalent elastic-plastic energy method as it has been done also by [55], a widely accepted approach for defining the transition between elastic and inelastic behavior. The ultimate displacement and load were identified at the point where the load-carrying capacity had decreased by approximately 85% from its peak, following the [54]. This reduction represents the onset of significant structural degradation, where the frame's ability to sustain loads diminishes rapidly. The backbone curves also allowed for the development of a linearized approximation for each specimen, illustrated in Figure 13. This linearized backbone curve connects the key stages of the structural response—starting from the initial stiffness phase, progressing through yielding, reaching the peak load, and ultimately descending to the failure or ultimate point.

The backbone curve characteristics presented in Table 3, including yielding displacement (Δy), yielding load (Fy), peak displacement (Δp), peak load (Fp), ultimate displacement (Δu), and ultimate load (Fu), were obtained following well-established methodologies for assessing nonlinear structural behavior under cyclic loading. The yielding point was identified using the equivalent elastic-plastic energy method, as proposed by previous studies. This method determines the transition between elastic and inelastic behavior by equating the areas under the actual and idealized bilinear load-displacement curves. The peak point corresponds to the maximum force the frame could sustain before strength degradation occurred. The ultimate point was defined as the displacement at which the load-carrying capacity was reduced to 85% of the peak load, following recommendations from existing seismic assessment guidelines. These characteristic points were extracted from the skeleton curve, which was derived by connecting the extreme values of the force-displacement relationship recorded in the hysteresis loops at each loading cycle. This approach ensures a robust evaluation of the structural response and enables comparisons between different frame configurations.

The analysis of these backbone curves reveals a substantial improvement in the load-carrying capacity due to the inclusion of concrete block infill masonry walls. The infill masonry walls played a crucial role in enhancing the structural performance at all stages of loading. For example, at the yielding point, the load-carrying capacity for frames in Group C increased by between 174% and 291%, and by 265% to 350% for frames in Group D, compared to their counterparts without infill masonry walls. This early-stage strength gain reflects the stiffening effect provided by the infill masonry walls, which effectively reduces the drift and deformation during initial loading. As the loading continued, this benefit persisted at the peak point, where the load-carrying capacity further increased by 267% to 441% for Group C, and 360% to 553% for Group D. The considerable improvement in peak load suggests that the infill masonry walls significantly delayed the onset of major structural damage, allowing the

frame to bear higher loads before reaching its maximum capacity. At the ultimate point, after the structure had undergone significant degradation, the load-carrying capacity was still substantially enhanced by 212% to 424% for Group C, and 272% to 325% for Group D, underscoring the lasting impact of the infill masonry walls in prolonging the structure's ability to carry loads even after severe damage had occurred.

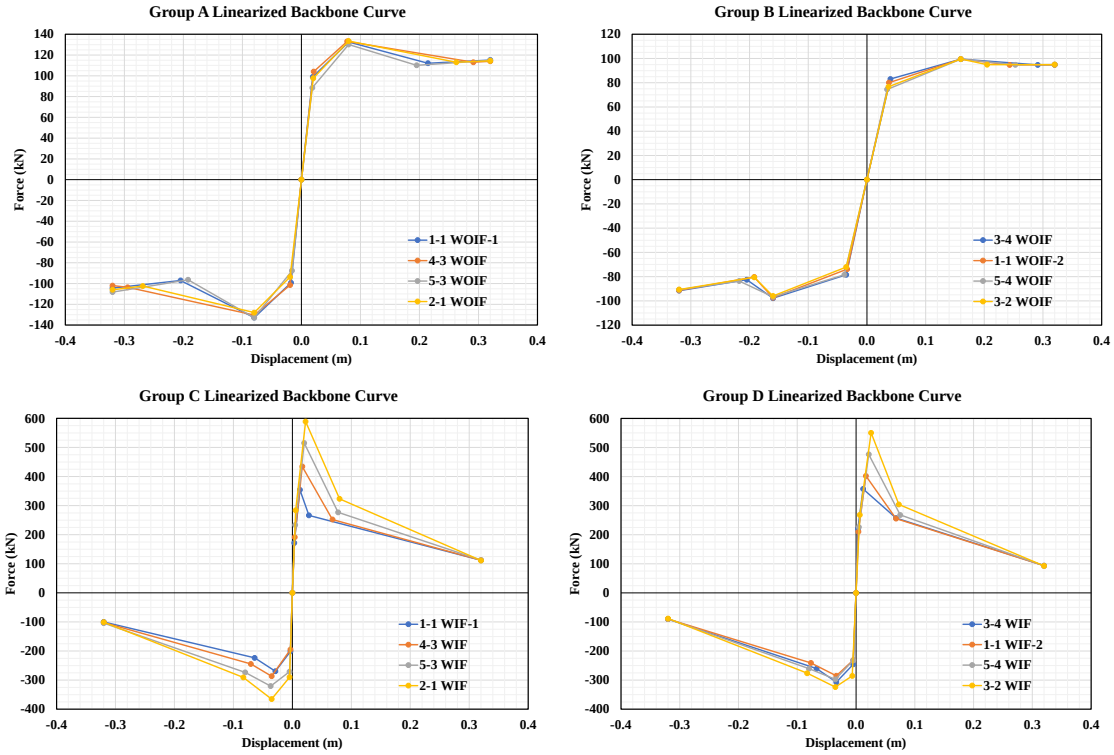

Figure 13. Linearized backbone curves for All 16 specimens across four groups (A, B, C, D).

Table 3. Characteristic points of backbone curve.

Specimens	Group	Yield Point		Peak Point		Ultimate Point	
		Δ_y/m	F_y/kN	Δ_p/m	F_p/kN	Δ_u/m	F_u/kN
1-1 WOIF-1	A	0.0192	98.95	0.0800	132.57	0.2144	112.10
4-3 WOIF		0.0208	104.03	0.0776	133.12	0.2912	113.08
5-3 WOIF		0.0184	88.51	0.0800	130.16	0.1952	110.12
2-1 WOIF		0.0200	97.63	0.0800	133.46	0.2624	113.03
3-4 WOIF	B	0.0400	83.03	0.1600	99.46	0.2912	94.70
1-1 WOIF-2		0.0376	80.06	0.1600	99.51	0.2432	94.71
5-4 WOIF		0.0344	74.48	0.1600	99.50	0.2528	94.83
3-2 WOIF		0.0368	76.71	0.1600	99.55	0.2048	94.90
1-1 WIF-1	C	0.0032	171.80	0.0128	354.20	0.0136	237.84
4-3 WIF		0.0040	191.44	0.0168	434.36	0.0176	274.41
5-3 WIF		0.0048	233.24	0.0200	515.17	0.0208	312.63
2-1 WIF		0.0056	283.81	0.0224	589.07	0.0232	479.11
3-4 WIF	D	0.0032	220.35	0.0120	357.60	0.0136	275.39
1-1 WIF-2		0.0040	210.44	0.0168	402.16	0.0184	257.70
5-4 WIF		0.0048	226.50	0.0216	476.50	0.0224	275.16
3-2 WIF		0.0064	268.25	0.0256	550.51	0.0272	308.29

Although the aspect ratio had a relatively limited effect on the frames without infill masonry walls, it had a pronounced influence on the frames with infill masonry walls. As the aspect ratio increased, effectively enlarging the infill masonry walls, the load-carrying capacity of the frames also increased. This is particularly noticeable in frames with higher story heights, such as those in Group D. These results demonstrate that larger infill masonry walls not only provide greater stiffness and strength but also contribute to more favorable load-distribution patterns within the frame, leading to enhanced structural performance under cyclic loading. Group D, with a higher story height of 4 meters, exhibited a larger percentage increase in load-carrying capacity compared to Group C, which had a story height of 3 meters. This suggests that the height of the frame influences the interaction between the frame and the infill masonry walls, particularly in terms of shear transfer and load distribution.

Interestingly, despite Group D exhibiting a greater overall increase in the percentage of load-carrying capacity, the peak load-bearing capacity of Group C was superior. This could be attributed to the relatively lower height of Group C, which results in a stiffer system that can resist higher peak loads before significant deformations occur. The frames in Group C, with their smaller height-to-width ratios, may experience a more efficient load transfer mechanism during the peak load phase, allowing them to achieve higher maximum loads before the onset of failure. In contrast, the taller frames in Group D, while benefiting from the increased height in terms of overall capacity, may be more susceptible to larger deformations, which could explain the relatively lower peak load compared to Group C.

3.3 Scant stiffness and degradation

Stiffness, in the context of structural engineering, refers to the ability of a structure to resist deformation under applied loads. It is a critical parameter that influences the behavior of a structure under seismic or cyclic loading conditions. The degradation of stiffness, which occurs as the structure undergoes repeated loading cycles, is a key indicator of structural damage and reduced load-carrying capacity over time. Secant stiffness is defined as the ratio of the sum of the absolute forces in both positive and negative loading directions to the corresponding absolute displacement in the same directions. This method of analysis provides a clear and consistent metric for tracking changes in stiffness throughout the loading process [54].

The degradation of secant stiffness for all specimens, measured under varying loading displacement levels across eight cycles, is presented in Figure 14. The abscissa (horizontal axis) represents the number of loading cycles, while the ordinate (vertical axis) represents the secant stiffness at each cycle. The introduction of infill masonry walls had a profound effect on the initial stiffness of the RC frame structures. The presence of infill masonry walls increased the initial stiffness by a factor of two to four compared to frames without infill masonry walls. This substantial enhancement can be attributed to the added rigidity provided by the infill masonry walls, which effectively limits initial deformations during the early stages of loading. The effect of aspect ratio was also significant; as the width-to-height ratio of the frame increased, so did the stiffness of the system. This relationship between aspect ratio and stiffness was evident in both the hysteresis curves and the backbone curves, where frames with larger aspect ratios demonstrated greater resistance to deformation.

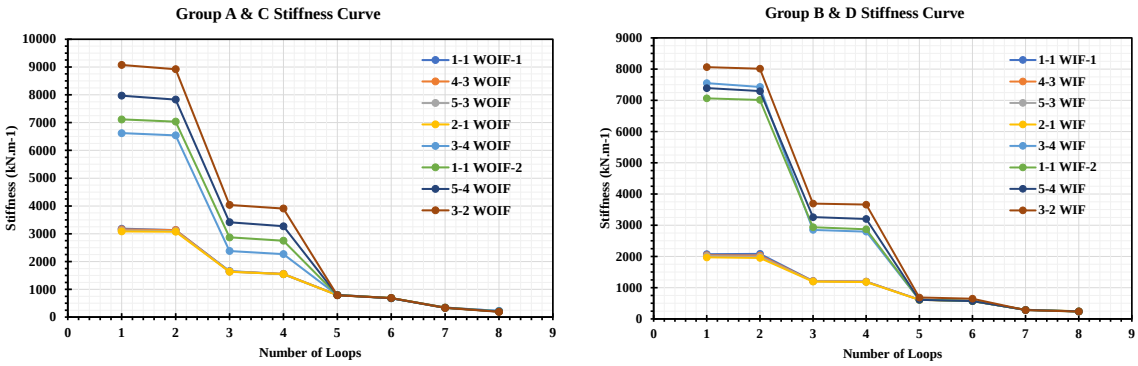

Figure 14. Secant Stiffness Degradation over eight loading cycles for all specimens.

In addition to the influence of aspect ratio, the story height of the frames also played a critical role in stiffness behavior. The group B and D exhibited greater initial stiffness than the group A and C. This difference can be attributed to the increased height of the infill masonry wall panels in the taller frames, which provided greater lateral resistance and contributed to the overall rigidity of the system. The increased height of the infill masonry walls in Group D enhanced the interaction between the frame and the infill masonry wall panel, leading to higher stiffness values compared to Group C.

Despite the significant increase in initial stiffness provided by the infill masonry walls, the rate of stiffness degradation over the course of cyclic loading was noticeably faster in specimens with infill masonry walls

compared to those without. This accelerated stiffness degradation is evident in both the stiffness curves and the hysteresis curves. As the frames with infill masonry walls underwent repeated cycles of loading, the interaction between the infill wall and the RC frame led to progressive stiffness degradation and energy dissipation, as represented by the macroelement model. These effects reflect the global response of the infill system under cyclic loading, including strength reduction and hysteresis pinching, rather than explicit localized damage mechanisms (e.g., block cracking or crushing), which led to a reduction in stiffness as the structure lost its ability to resist further deformations. Consequently, the secant stiffness values dropped more rapidly in frames with infill masonry walls as loading cycles increased, particularly after reaching the peak load. Frames without infill masonry walls, on the other hand, experienced a more gradual decline in stiffness. While these frames did not benefit from the initial stiffness boost provided by infill masonry wall, they demonstrated greater resilience in maintaining their stiffness throughout cyclic loading. The slower rate of stiffness degradation in these frames can be attributed to their simpler load-resisting mechanism, which relied primarily on the flexural behavior of the RC columns and beams, without the additional complexities introduced by the interaction between the frame and infill masonry walls.

3.4 Energy dissipation

The energy dissipation capacity of the system under cyclic loading is illustrated in Figure 15. This energy dissipation is calculated as the cumulative area enclosed by the hysteresis loops at each loading stage, representing the total energy absorbed by the system. The energy dissipated is primarily due to various mechanisms within the structure, including cracking of the concrete, yielding of the steel reinforcement, crushing of the infill masonry wall, and frictional effects between structural elements. As the loading progresses and these mechanisms intensify, the system dissipates more energy, reflecting its ability to resist damage and absorb seismic forces.

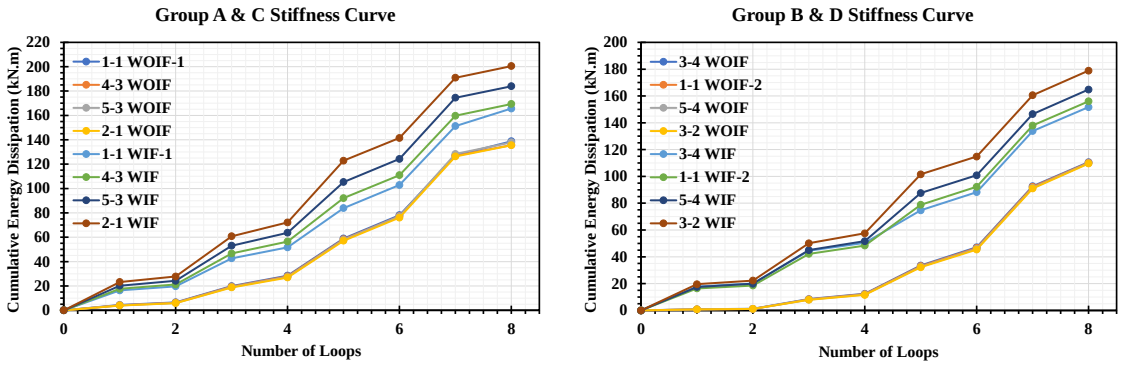

Figure 15. Cumulative energy dissipation curve over eight loading cycles for all specimens.

The results demonstrate that the presence of infill masonry walls plays a significant role in increasing the system's energy dissipation capacity. Infill masonry walls contribute to energy dissipation by undergoing cracking and crushing during cyclic loading, thereby absorbing and dissipating a portion of the input energy. Consequently, systems with infill masonry walls exhibited higher levels of energy consumption compared to systems without infill masonry walls, as evidenced by the cumulative energy dissipation curves. These curves reveal that the infill masonry walls help to mitigate the effects of cyclic loading by absorbing a substantial portion of the energy, which would otherwise be concentrated in the RC frame.

Furthermore, the size and configuration of the infill masonry wall have a direct impact on the amount of energy dissipated by the system. Increasing the height of the infill masonry wall, as well as adjusting the aspect ratio (width-to-height ratio) of the frames, resulted in greater energy dissipation. This is particularly evident in systems with taller frames and larger aspect ratios, where the increased size of the infill masonry wall provides more surface area for energy dissipation through cracking and crushing mechanisms. The results indicate that the larger the infill masonry wall, the more energy is dissipated during the loading process, which helps to reduce the overall demand on the RC frame and delay the onset of failure.

The cumulative energy dissipation curves provide valuable insight into the structural performance of RC frames under seismic conditions. Systems with infill masonry walls not only exhibit greater initial stiffness and load-carrying capacity but also demonstrate enhanced energy dissipation, making them more effective at withstanding seismic forces. However, this increased energy dissipation also correlates with more significant damage to the infill masonry walls, which can lead to faster degradation of the system’s overall stiffness and strength. Nonetheless, the ability of infill masonry walls to dissipate energy plays a crucial role in improving the resilience of the structure and mitigating damage during seismic events.

3.5 Ductility coefficient

Figure 16 presents the ductility coefficients for all the specimens. The ductility coefficient is defined as the ratio of the ultimate deformation to the yielding deformation and provides a critical measure of the structure's capacity to undergo large deformations without losing its load-carrying capacity. The results indicate a clear trend: the introduction of infill masonry walls significantly reduces the ductility coefficient of the RC frame system. This reduction in ductility aligns with findings reported in previous studies, such as those by [56], where it was observed that the inclusion of stiff infill masonry wall elements constrains the deformation capacity of the frame.

In this study, the addition of infill masonry walls resulted in a notable reduction in ductility. Generally, for Group C, which consists of frames with a 3-meter story height, the ductility coefficient decreased by 31% to 41% when compared to the frames without infill masonry walls. Group D, with a 4-meter story height, experienced an even more significant reduction in ductility, ranging from 58% to 78%. This substantial decrease can be attributed to the interaction between the RC frame and the infill masonry walls, which limits the overall flexibility of the system and leads to earlier onset of cracking and localized failure mechanisms, thereby constraining the frame's ability to undergo large deformations. While the aspect ratio of the frame (width-to-height ratio) had only a minor effect on the ductility coefficient, the height of the infill masonry wall emerged as a critical factor. Taller infill masonry walls, such as those in Group D, contributed to a more pronounced reduction in ductility compared to shorter infill masonry walls in Group C. This behavior can be explained by the increased stiffness and rigidity of taller infill masonry walls, which exacerbates the interaction between the frame and the infill masonry walls, causing earlier yielding and limiting the deformation capacity of the structure. The greater the height of the infill masonry wall, the more it restricts the frame's ability to deform plastically, leading to a sharper decline in ductility.

The reduced ductility in systems with infill masonry walls is a significant consideration in seismic design, as ductility is a key parameter in a structure's ability to absorb and dissipate energy during earthquake-induced cyclic loading. Although infill masonry walls enhance the initial stiffness and strength of the frame, their detrimental effect on ductility suggests that careful attention must be paid to balancing these opposing characteristics when designing RC frames for seismic resilience. The reduction in ductility highlights the trade-off between increased stiffness and load-carrying capacity versus the ability of the structure to undergo large, inelastic deformations without collapse.

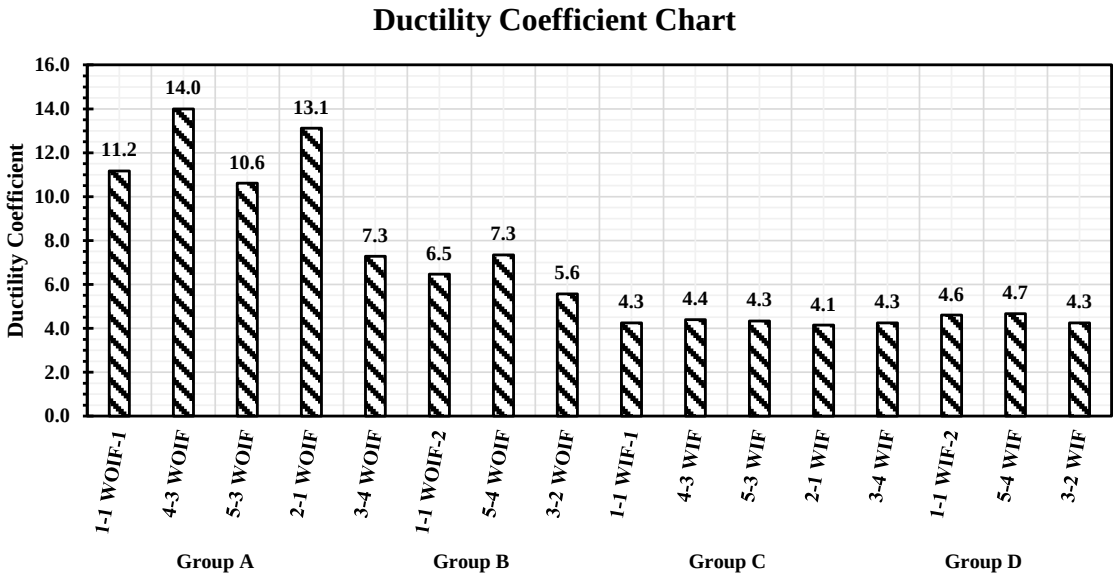

Figure 16. Ductility coefficient chart.

While infill masonry walls significantly enhance the load-carrying capacity and energy dissipation of RC frames, their inclusion introduces several drawbacks that must be carefully considered in seismic design. One major limitation is the increased brittleness of the system, as infill walls reduce the ductility of the frame by up to 78%, particularly in taller structures. This brittleness can lead to sudden and catastrophic failure under extreme loading conditions. Additionally, infill walls contribute to rapid stiffness degradation during cyclic loading, as evidenced by the pronounced pinching and narrowing of hysteresis loops in frames with infills (Figures 10–11). This degradation reduces the system’s ability to sustain repeated seismic demands and may exacerbate damage progression.

3.6 Comparison with prior studies

The findings of this study align with and extend existing research on infilled RC frames while highlighting critical distinctions due to the use of modern large-format concrete blocks and geometric variations. For instance, the observed increase in load-carrying capacity (267–553%) with infill walls corroborates trends reported for traditional masonry infills, such as the 200–400% enhancements documented by [6] for clay brick systems. However, the higher capacity gains here likely stem from the superior compressive strength and stiffness of concrete blocks compared to clay-based infills, as noted in full-scale masonry studies [17,32].

The rapid stiffness degradation and ductility reduction (31–78%) observed in infilled frames mirror trends in prior studies, such as the work of [15] on AAC masonry and [56] on high-strength frames. However, taller frames (Group D) exhibited more severe degradation than reported in earlier research, likely due to amplified out-of-plane effects not explicitly modeled here. This distinction highlights the critical role of story height, a parameterless emphasized in studies focused on low-rise systems [26]. Furthermore, the pinched hysteresis loops and brittle energy dissipation patterns reflect the inherent brittleness of concrete blocks, diverging from the fuller hysteresis loops of ductile clay brick systems [55]. Such findings challenge conventional design assumptions that treat infill materials as interchangeable.

Finally, the study's results underscore a critical trade-off in infilled frame design: while modern concrete blocks enhance strength and energy dissipation, they exacerbate ductility loss and stiffness degradation, particularly in taller frames. This contrasts with earlier work on smaller-unit masonry, which prioritized material ductility over strength [48]. The synthesis of these findings suggests that contemporary construction practices—using large-format blocks and taller geometries—demand revised design strategies to balance strength and deformability. For instance, retrofitting techniques such as flexible mortar joints or partial-height infills [28] could mitigate brittleness while retaining strength benefits. By bridging gaps between traditional and modern infill systems, this work advances the understanding of seismic performance in evolving construction contexts.

4. Conclusions

This study tested how infill masonry walls and frame geometry—like aspect ratios and story heights—affect concrete buildings' earthquake resilience. By analyzing frames with and without infills under cyclic loads, we found that infill walls tripled load capacity but cut ductility by up to 78%, especially in taller frames. Wider bays (higher aspect ratios) softened this trade-off, balancing strength and energy absorption. These results challenge designers to rethink how infills are integrated: their benefits are undeniable, but their risks demand careful mitigation. Two sets of frames were categorized and studied: Group A and Group C, with a story height of 3 meters, and Group B and Group D, with a story height of 4 meters. Aspect ratios were varied from 0.75 to 2 in both cases, allowing for a thorough analysis of their effects on frame behavior. The main findings and conclusions can be summarized as follows:

1) Bare frames showed consistent hysteresis behavior regardless of aspect ratio, confirming that geometry alone has limited influence on their seismic performance. Introducing infill walls, however, transformed this response: shorter frames in Group C (3m story height) with infills achieved marginally higher load capacities than taller ones in Group D (4m), but both exhibited similar energy dissipation patterns. This underscores how infills redistribute forces, making story height—not just aspect ratio—a critical factor in strength outcomes.

2) The similarity in hysteresis curves across different aspect ratios highlights the resilience of frames without infill masonry walls under cyclic loading. This finding is consistent with previous experimental studies by [53], which demonstrated that geometric properties alone are not always the dominant factor in determining the load-carrying capacity of bare RC frames. The study further affirms that other variables, such as material properties and boundary conditions, may play more significant roles in influencing the seismic response of bare RC frames.

3) The presence of infill masonry walls in RC frames introduced significant changes to the hysteresis behavior. Frames with infill masonry walls exhibited more pinched hysteresis curves, indicative of greater energy dissipation and nonlinear behavior during cyclic loading. This behavior was most evident in frames with higher aspect ratios, where the interaction between the frame and the infill masonry walls led to greater stiffness degradation and increased energy absorption.

4) The study showed that infill masonry walls significantly improve the load-carrying capacity of RC frames, particularly when the width-to-height aspect ratio is increased. For instance, in frames from Group C (3-meter story height) and Group D (4-meter story height), the inclusion of infill masonry walls led to notable increases in both stiffness and strength, with the effect being more pronounced in frames with higher aspect ratios. This can be attributed to the increased bracing provided by the infill masonry walls, which enhance the overall structural integrity of the frame.

5) Additionally, the comparison between specimens with different story heights (e.g., 3 meters in Group C vs. 4 meters in Group D) revealed that the height of the infill masonry walls has a direct impact on the hysteresis behavior. Taller infill masonry walls contributed to more significant stiffness degradation and greater load-carrying

capacity, which can be explained by the increased vertical load that these walls support during seismic events. These findings align with the experimental results reported by [54], who also observed a strong correlation between infill masonry wall height and structural performance under cyclic loading.

6) Aspect ratio, defined as the width-to-height ratio of the frame, emerged as a critical parameter influencing the load-carrying capacity and hysteresis behavior of RC frames. For frames with infill masonry wall, increasing the aspect ratio was found to have a substantial effect on the load-carrying capacity. Frames with larger aspect ratios exhibited higher load-carrying capacity and greater resistance to seismic forces, particularly in the case of infill masonry wall frames. This can be attributed to the increased lateral stiffness provided by the wider frame geometry, which enhances the ability of the structure to withstand lateral displacements during earthquakes.

7) In contrast, for frames without infill masonry walls, the impact of aspect ratios was less pronounced. Although larger aspect ratios led to marginal increases in load-carrying capacity, the overall effect was relatively small compared to the frames with infill masonry walls. This suggests that while geometric properties play a role in determining the seismic performance of RC frames, the presence of infill masonry walls amplifies the importance of aspect ratios in the design and evaluation of structural systems.

The importance of this study lies in its detailed exploration of the combined effects of frame geometry and infill masonry walls on the seismic performance of RC structures. The findings contribute significantly to the understanding of how RC frames behave under cyclic loading, particularly in earthquake-prone areas where structural resilience is critical. By providing insights into the hysteresis behavior of both bare and infill masonry wall frames, this study offers valuable guidance for engineers and researchers involved in the design, assessment, and retrofitting of RC structures. One of the key contributions of this research is the identification of the role those geometric properties, specifically aspect ratios and infill masonry wall height, play in influencing the seismic performance of RC frames. This information is vital for structural engineers who are tasked with designing buildings that can withstand seismic forces, as it highlights the need for careful consideration of both frame geometry and the presence of infill masonry walls in the design process. Furthermore, the study's findings have important implications for the retrofitting of existing RC structures. Many older buildings were constructed without sufficient consideration of seismic forces, and the insights gained from this research can be applied to improve the performance of such structures through the strategic use of infill masonry walls and geometric modifications. For engineers, this underscores the need to optimize infill design in earthquake-prone regions. Retrofitting existing structures with partial-height infills or flexible mortar joints could improve safety without sacrificing ductility. New constructions should prioritize moderate aspect ratios (e.g., 1.5–2.0) to leverage stiffness while maintaining deformability. Simple fixes like reinforcing frame-infill interfaces or using lighter masonry blocks could further enhance performance.

Future research could build on these results by conducting experimental validations, investigating different infill materials, examining multi-story frames, and developing cost-effective design guidelines that incorporate the observed effects of aspect ratio and infill walls. Additionally, studying the long-term performance of RC frames with infill walls under repeated seismic events could provide valuable insights for sustainable structural design. Overall, this study contributes significantly to the understanding of RC frame behavior under cyclic loading and offers crucial guidance for enhancing building safety in earthquake-prone regions. Moreover, Future work should explore innovative infill materials—such as fiber-reinforced polymers or aerated concrete—to reduce brittleness while preserving strength. Multi-story buildings, which face compounded risks from out-of-plane forces and repeated aftershocks, also warrant urgent study. Field validation of these findings through real-world retrofits or shake-table tests would bridge the gap between lab models and lifesaving designs.

5. References

[1] El-Dakhakhni W, Hamid A, Hakam Z, Elgaaly M. Hazard mitigation and strengthening of unreinforced masonry walls using composites. Composite Structures. 2006;73(4):458-477.
[2] Chaker AA, Cherifati A. Influence of masonry infill panels on the vibration and stiffness characteristics of R/C frame buildings. Earthquake Engineering & Structural Dynamics. 1999;28(9):1061-1065.
[3] Lieping Y, Xinzheng L, Zhe Q, Peng F. Analysis on building seismic damage in the Wenchuan earthquake. In: The 14th World Conference on Earthquake Engineering. 2008.
[4] Yan PL, Sun BT, Zhang HY. Seismic damage to RC frame teaching building in Lushan MS7.0 earthquake. China Civil Engineering Journal. 2014;47:24-28.
[5] Chiou YJ, Tzeng JC, Liou YW. Experimental and analytical study of masonry infilled frames. Journal of Structural Engineering. 1999;125(10):1109-1117.
[6] Mehrabi AB, Shing PB, Schuller M, Noland J. Experimental evaluation of masonry-infilled RC frames. Journal of Structural Engineering. 1996;122(3):228-237.
[7] Shan S, Li S, Xu S, Xie L. Experimental study on the progressive collapse performance of RC frames with infill walls. Engineering Structures. 2016;111:80-92.

[8] Jiang H, Mao J, Liu X. Experimental study on seismic performance of masonry infilled RC frame with different types of connections. Journal of Building Structures. 2014;35:60-67.
[9] Mehrabi AB, Benson Shing P, Schuller MP, Noland JL. Experimental evaluation of masonry-infilled RC frames. Journal of Structural Engineering. 1996;122:228-237.
[10] Kakaletsis D, Karayannis C. Experimental investigation of infilled r/c frames with eccentric openings. Structural Engineering and Mechanics. 2007;26:231-250.
[11] Kakaletsis DJ, Karayannis CG. Experimental investigation of infilled reinforced concrete frames with openings. ACI Structural Journal. 2009;106:132-141.
[12] Tasnimi AA, Mohebkhah A. Investigation on the behavior of brick-infilled steel frames with openings, experimental and analytical approaches. Engineering Structures. 2011;33:968-980.
[13] Mansouri A, Marefat MS, Khanmohammadi M. Experimental evaluation of seismic performance of low-shear strength masonry infills with openings in reinforced concrete frames with deficient seismic details. Structural Design of Tall and Special Buildings. 2014;23:1190-1210.
[14] Sigmund V, Penava D. Influence of openings, with and without confinement, on cyclic response of infilled R-C frames—An experimental study. Journal of Earthquake Engineering. 2014;18:113-146.
[15] Schwarz S, Hanaor A, Yankelevsky DZ. Experimental response of reinforced concrete frames with AAC masonry infill walls to in-plane cyclic load. Structures. 2015;3:306-319.
[16] Sidi S, Li S, Xu SY, Xie L. Experimental study on the progressive collapse performance of RC frames with infill walls. Engineering Structures. 2016;111:80-92.
[17] Li S, Shan S, Zhai C, Xie L. Experimental and numerical study on progressive collapse process of RC frames with full-height infill walls. Engineering Failure Analysis. 2016;59:57-68.
[18] Varum H, Furtado A, Rodrigues H, Dias-Oliveira J, Vila-Pouca N, Arêde A. Seismic performance of the infill masonry walls and ambient vibration tests after the Ghorka 2015, Nepal earthquake. Bulletin of Earthquake Engineering. 2017;15:1185-1212.
[19] Stavridis A, Shing PB. Finite-element modeling of nonlinear behavior of masonry-infilled RC frames. Journal of Structural Engineering. 2010;136(3):285-296.
[20] Koutromanos I, Stavridis A, Shing PB, Willam K. Numerical modeling of masonry-infilled RC frames subjected to seismic loads. Computers & Structures. 2011;89(11-12):1026-1037.
[21] Dolatshahi KM, Aref AJ. Two-dimensional computational framework of meso-scale rigid and line interface elements for masonry structures. Engineering Structures. 2011;33(12):3657-3667.
[22] Moaveni B, Stavridis A, Lombaert G, Conte JP, Shing PB. Finite-element model updating for assessment of progressive damage in a 3-story infilled RC Frame. Journal of Structural Engineering (United States). 2013;139(10):1665-1674.
[23] Asteris PG, Cotsovos DM, Chrysostomou CZ, Mohebkhah A, Al-Chaar GK. Mathematical micromodeling of infilled frames: state of the art. Engineering Structures. 2013;56:1905-1921.
[24] Bahreini V, Mahdi T, Najafizadeh M. Numerical study on the in-plane and out-of-plane resistance of brick masonry infill panels in steel frames. Shock and Vibration. 2017;2017.
[25] Chen X, Liu Y. Numerical study of in-plane behaviour and strength of concrete masonry infills with openings. Engineering Structures. 2015;82:226-235.
[26] Furtado A, Rodrigues H, Arêde A, Varum H. Simplified macro-model for infill masonry walls considering the out-of-plane behaviour. Earthquake Engineering & Structural Dynamics. 2016;45:507-524.
[27] Yuen YP, Kuang JS. Nonlinear seismic responses and lateral force transfer mechanisms of RC frames with different infill configurations. Engineering Structures. 2015;91:125-140.
[28] Facconi L, Minelli F. Retrofitting RC infills by a glass fiber mesh reinforced overlay and steel dowels: experimental and numerical study. Construction and Building Materials. 2020;231:117133.
[29] Mosalam K, Günay S. Progressive collapse analysis of reinforced concrete frames with unreinforced masonry infill walls considering in-plane/out-of-plane interaction. Earthquake Spectra. 2015;31:921-943.
[30] Chiozzi A, Miranda E. Fragility functions for masonry infill walls with in-plane loading. Earthquake Engineering & Structural Dynamics. 2017;46:2831-2850.
[31] Baghi H, Oliveira A, Cavaco E, Neves L, Júlio E. Experimental testing of RC frames with masonry infills subjected to a column failure. In: 5th International Conference on Integrity-Reliability-Failure. Faculty of Engineering/U. Porto; 2016.
[32] Zhai C, Kong J, Wang X, Chen Z. Experimental and finite element analytical investigation of seismic behavior of full-scale masonry infilled RC frames. Journal of Earthquake Engineering. 2016;20:1171-1198.
[33] Di Trapani F, Macaluso G, Cavaleri L, Papia M. Masonry infills and RC frames interaction: literature overview and state of the art of macromodeling approach. European Journal of Environmental and Civil Engineering. 2015;19:1059-1095.
[34] Mucedero G, Perrone D, Monteiro R. Infill variability and modelling uncertainty implications on the seismic loss assessment of an existing RC Italian school building. Applied Sciences. 2022;12(23):12002.

[35] Mohamed H, Skoulidou D, Romão X. Quantification of the effects of different uncertainty sources on the seismic fragility functions of masonry-infilled RC frames. Structures. 2023;50:1069-1088.
[36] De Risi MT, Di Domenico M, Ricci P, Verderame GM, Manfredi G. Experimental investigation on the influence of the aspect ratio on the in-plane/out-of-plane interaction for masonry infills in RC frames. Engineering Structures. 2019;189:523-540.
[37] Papasotiriou A, Athanatopoulou A, Kostinakis K. Parametric study of the masonry infills' effect on the seismic performance of R/C frames based on the use of different damage measures. Engineering Structures. 2021;241:112326.
[38] Guettala S, Abdesselam I, Chebili R, Guettala S. Assessment of the effects of infill walls' layout in plan and/or elevation on the seismic performance of 3D reinforced concrete structures. Asian Journal of Civil Engineering. 2023;25:657-673.
[39] Abdesselam I, Guettala S, Zine A. Fiber-based modeling for investigating the existence of a soft storey for masonry infilled reinforced concrete structures. Asian Journal of Civil Engineering. 2024;25:1949-1965.
[40] Guettala S, Khelaifia A, Chebili R, Guettala S. Effect of infill walls on seismic performance of multi-story buildings with shear walls. Asian Journal of Civil Engineering. 2024;25:3989-3999.
[41] Mucedero G, Perrone D, Monteiro R. Infill variability and modelling uncertainty implications on the seismic loss assessment of an existing RC Italian school building. Applied Sciences. 2022;12(23):12002.
[42] Mohamed H, Skoulidou D, Romão X. Quantification of the effects of different uncertainty sources on the seismic fragility functions of masonry-infilled RC frames. Structures. 2024;50:1069-1088.
[43] Milanesi RR, Morandi P, Magenes G. Local effects on RC frames induced by AAC masonry infills through FEM simulation of in-plane tests. Bulletin of Earthquake Engineering. 2018;16(9):4053-4080.
[44] Donà M, Minotto M, Verlato N, Da Porto F. A new macro-model to analyse the combined in-plane/out-of-plane behaviour of unreinforced and strengthened infill walls. Engineering Structures. 2021;250:113487.
[45] Seismosoft. SeismoStruct V24. 2024.
[46] Mander JB, Priestley MJN, Park R. Theoretical stress-strain model for confined concrete. Journal of Structural Engineering. 1988;114(8):1804-1826.
[47] Madas P. Advanced modelling of composite frames subjected to earthquake loading [PhD Thesis]. Imperial College, University of London; 1993.
[48] Madas P, Elnashai AS. A new passive confinement model for transient analysis of reinforced concrete structures. Earthquake Engineering and Structural Dynamics. 1992;21:409-431.
[49] Martínez-Rueda JE, Elnashai AS. Confined concrete model under cyclic load. Matériaux Et Constructions. 1997;30(3):139-147.
[50] Crisafulli FJ. Seismic behaviour of reinforced concrete structures with masonry infills [PhD Thesis]. University of Canterbury; 1997.
[51] Scott MH, Fenves GL. Plastic hinge integration methods for force-based beam–column elements. Journal of Structural Engineering. 2006;132(2):244-252.
[52] Calabrese A, Almeida JP, Pinho R. Numerical issues in distributed inelasticity modeling of RC frame elements for seismic analysis. Journal of Earthquake Engineering. 2010;14(sup1):38-68.
[53] Hemmati A, Kheyroddin A, Farzad M. Experimental study of reinforced concrete frame rehabilitated by concentric and eccentric bracing. DOAJ (DOAJ: Directory of Open Access Journals). 2020.
[54] Wang F, Zhao K, Zhang J, Yan K. Influence of different types of infill walls on the hysteretic performance of reinforced concrete frames. Buildings. 2021;11(7):310.
[55] Tang X, Cai J, Chen Q, Liu X, He A. Seismic behaviour of through-beam connection between square CFST columns and RC beams. Journal of Constructional Steel Research. 2016;122:151-166.
[56] Essa AS, Badr MRK, El-Zanaty AH. Effect of infill wall on the ductility and behavior of high strength reinforced concrete frames. HBRC Journal. 2014;10(3):258-264.